

## SOOT PARTICLE SIZE DISTRIBUTION NEAR THE CYLINDER WALL IN A DIRECT INJECTION DIESEL ENGINE

M. A. ZUBER, W. M. F. WAN MAHMOOD\*, Z. HARUN, Z. Z. ABIDIN

Department of Mechanical and Materials Engineering,  
Faculty of Engineering and Built Environment, Universiti Kebangsaan Malaysia,  
43600 UKM Bangi, Selangor, Malaysia

\*Corresponding Author: faizal.mahmood@ukm.edu.my

### Abstract

Investigation of soot particle size and its distribution inside a direct injection diesel engine provides the idea of how soot particles are distributed in an engine cylinder, particularly near the cylinder wall. The objective of the present study is to obtain soot particles size distribution near the cylinder wall which contributes to the issue of soot in lubricating oil. The study was performed numerically by post-processing CFD simulation data with in-house Matlab routines. Hiroyasu soot formation, Nagle & Strickland-Constable oxidation and Wersborg soot coagulation models were adapted to calculate the soot particle size in this study. Soot particle size calculation, which was carried out post-processed, reduced the simulation time and computational effort. Results obtained showed that soot particles with a size smaller than 50 nm were found in the squish region particularly near the cylinder wall. As much as five percent of the total number of soot particles tracked were found in the boundary layer at the cylinder wall.

Keywords: CFD, Coagulation, Particle tracking, Soot size distribution, Squish region.

### 1. Introduction

Soot produced during the combustion inside diesel engine cylinder is capable of contaminating and degrading the engine oil, which would accelerate the engine wear and tear [1-3]. The mechanisms of soot particle transfer to the wall boundary are not entirely understood and the properties of soot particle that transferred to the wall boundary are likewise unclear.

The transport mechanism of soot particle to the wall boundary had been conducted in a series of computational fluid dynamics (CFD) simulation [4, 5]. The main reason for soot transfer near to the wall boundary is caused mainly by the thermo-

**Nomenclatures**

$E_{sf}$	Activation Energy
$K$	Coagulation coefficient
$k_A, k_B, k_T, k_Z$	Empirical rate constant for NSC soot oxidation mechanism
$k_1, k_2, k_3, k_4$	Slopes for the use of Runge-Kutta method
$M_{fvi}$	Mass of fuel vapour
$M_{sfi}$	Mass of soot formed
$N$	Soot particle formation multiplication factor
$n$	Soot particle number density
$P$	Pressure
$R$	Universal Gas Constant
$\dot{R}_{NSC}$	Rate of soot oxidation based on NSC mechanism
$s$	Distance
$s_n$	Soot particle position
$s_{n+1}$	Soot particle position at the next time step
$T$	Temperature
$u$	Velocity vector

**Greek Symbols**

$\Delta t$	Time step interval
------------	--------------------

**Abbreviations**

ATDC	After Top Dead Center
CA	Crank angle
CFD	Computational Fluid Dynamics
NSC	Nagle & Strickland-Constable

phoresis effect rather than blowby [5], where the difference of temperature between the cylinder wall and combustion temperature inside the cylinder forces the soot, specifically soot near the wall boundary layer, to migrate to the wall or oil film. Soot that entrapped in this area will have the tendency to stick to the wall and scraped down by the piston into the crankcase and deposited in the engine oil.

Therefore, an investigation on soot movement and properties inside an engine cylinder at various crank angle degrees are desirable. In the previous investigation, Wan Mahmood et al. [6] reported the soot particle pathlines from selected initial local points of interest to the soot particle locations at a given crank angle (CA). Zuber et al. [7, 8] reported soot particle size distribution in squish region and the whole cylinder taking into accounts of soot surface growth and soot oxidation processes. These have provided insights of soot movement inside the cylinder especially near the cylinder wall as well as soot size distribution at that instance. Obtaining accurate soot size distribution near the cylinder wall, i.e., squish region, further analysis of mechanisms of transfer of soot to the wall can be performed. Accordingly, this paper reports the study of soot particle size distribution in the squish region which was obtained by considering the effect of soot oxidation, surface growth and coagulation on the size of the in-cylinder soot particles.

The present paper aimed to obtain the soot particle size distribution in the diesel engine. Using soot model based on Hiroyasu soot formation model, Nagle & Strickland-Constable oxidation model and Wersborg soot coagulation to calculate the soot particle size. While the soot particle movement inside the engine cylinder

was tracked by using Runge-Kutta 4th order numerical method, in which provide the distribution of soot particle in the entire engine cylinder at a time interval of 8-120° CA ATDC.

## 2. Soot Size Modelling

As reported by Rao and Honnery [9], two-step soot model by Hiroyasu and Nishida [10] required less computational cost and take shorter time to be solved in computational fluid dynamic (CFD) software compare the other models. Hiroyasu soot model only considers fuel vapour as soot precursor the soot formation whereas other detailed models such as 8-step model developed by Fusco et al. [11] and detailed soot model developed by Tao et al. [12] consider various chemical reactions and physical processes into account. The main drawback of Hiroyasu soot model is its inability to predict the soot particle size and its number density in comparison with other models.

In this research, we used a special method to calculate the size of soot particle size and its number density. Using post-processed CFD simulation data of in-cylinder combustion performed based on Hiroyasu soot model, prediction of soot particle size and soot number density can be obtained by using a numerical method. This method separates chemical and physical processes of the combustion as the soot particle size and soot number density were calculated based on the soot mass and other relevant data from the previous CFD simulation. This method was used to shorten the simulation time and reduce the computational effort.

In this paper, two-step soot model by Hiroyasu soot formation and Nagle & Strickland-Constables (NSC) oxidation model were used to simulate the evolution of soot due to surface growth and oxidation processes. Fuel injected and fragmented during the combustion was assumed to be converted to soot particle at specific engine conditions, for example, high temperature and high fuel concentration, and subsequently subjected to surface growth, oxidation and coagulation processes.

Calculation of soot particle size and number density was performed by using numerical method where the properties data of the soot particle at a given CA were obtain from the CFD results. Hiroyasu soot surface growth as in Eq. (1) was used to calculate the increase in mass due to soot surface growth while NSC oxidation in Eq. (2) was used to calculate the mass loss due to oxidation. Until this stage, the research was reported in the previous article [8]. In this report, an addition process of coagulation was introduced as another soot growth process where the soot particle grows due to combination of two or more soot particles into one larger particle and thus reduces soot number density. Calculating soot number density loss due to coagulation process was based on Eq. (3), adapted from Wersborg et al. [13].

$$\frac{dM_{sfi}}{dt} = NM_{fvi} P_i^{0.5} e^{-E_{sf}/RT_i} \quad (1)$$

$$\dot{R}_{NSC} = \frac{k_A p}{1 + k_Z p} x + k_B p(1 - x) \quad (2)$$

$$\dot{N}_c = \frac{1}{2} K n^2 \quad (3)$$

In Eq. (1),  $M_{fvi}$  represents the mass of fuel vapour, which was considered a source of soot,  $P$  is the pressure,  $N$  is the soot particle formation multiplication factor and  $T$  is the temperature.  $E_{sf}$ , equal to 12500 cal/mole, is the activation energy and gas constant  $R=1.987$  cal/mole-K. For Eq. (2),  $p$  represents the pressure and the values for  $k_A$ ,  $k_B$ ,  $k_T$  and  $k_Z$  can be calculated using Eqs. (4) to (7) with an assumption that the carbon surface has two sides, one with the reactive side with fraction value of  $x$  and other side is the less reactive with fraction value of  $1-x$ . While for Eq. (3),  $K$  represents the coagulation coefficient and  $n$  is the soot particle number density.

$$k_A = 20 \times e^{-30,000/RT} \text{ g cm}^{-2} \text{ s}^{-1} \text{ atm}^{-1} \quad (4)$$

$$k_B = 4.46 \times 10^{-3} \times e^{-15,200/RT} \text{ g cm}^{-2} \text{ s}^{-1} \text{ atm}^{-1} \quad (5)$$

$$k_T = 1.51 \times 10^5 \times e^{-97,00/RT} \text{ g cm}^{-2} \text{ s}^{-1} \quad (6)$$

$$k_Z = 21.3 \times e^{4,100/RT} \text{ atm}^{-1} \quad (7)$$

### 3. Soot Particle Tracking

In this report, the particle tracking method was based on previous work where the details of particle tracking are available [7]. Soot particle were tracked by using Runge-Kutta 4th order method as in Eq. (8). Where  $s_n$  represent the initial time step,  $s_{n+1}$  represent the next time step,  $\Delta t$  represent the time different and coefficient  $k$  represent the velocity of soot particle at given time as in Eqs. (9) to (11). Based on the location and in-cylinder data from CFD result, the soot particle trajectory was calculated to determine the location of soot particle. Using this method, the pathline of soot particle movement can be predicted along with the soot particle properties.

$$s_{n+1} = s_n + \frac{1}{6}(k_1 + 2k_2 + 2k_3 + k_4)\Delta t \quad (8)$$

$$k_2 = u\left(s_n + \frac{1}{2}\Delta t, t_n + \frac{1}{2}k_1\Delta t\right) \quad (9)$$

$$k_3 = u(s_n + \Delta t, t_n - k_1\Delta t + 2k_1\Delta t) \quad (10)$$

$$k_4 = u(s_n + \Delta t, t_n + k_3\Delta t) \quad (11)$$

## 4. Results and Discussion

### 4.1. Particle tracking

From the CFD simulation and post-processing via numerical method, soot particle size and soot particle pathlines were calculated and obtained. In general, the soot particle movement inside the engine cylinder follows the in-cylinder bulk gas movement in the direction of clockwise as seen in Fig. 1. This figure only showed representative numbers of soot particle pathlines from initial locations at 8° CA ATDC to final locations at 120° CA ATDC. The determination of 8° CA ATDC as

the starting crank angle for the calculation of soot movement and size was due to the fact that at that particular crank angle the soot produced was sufficiently abundant to start the tracking while before 8° CA ATDC, fewer soot particles available to be tracked. Following the soot particle movement showed that at 14° CA ATDC soot particles start to enter squish area and at 22° CA ATDC the soot particles move near the wall boundary.

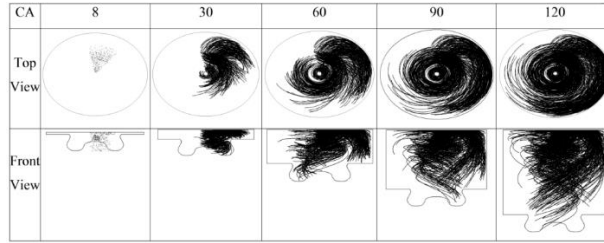


**Fig. 1. In-cylinder soot particle pathline following bulk gas swirl movement in clockwise direction.**

Figure 2 specifically shows the soot particle pathlines in squish region. Squish region is an area near the cylinder wall above the piston surface. Soot particle in squish region tends to stay there until the end of combustion. This shows that as soot particles enter the squish region, they tend to stay there and would probably stick to the cylinder wall. Soot particles in this area have the possibility to move near the cylinder wall by several transport mechanisms [4, 5] and thus subsequently scraped by the piston ring into the crank case.

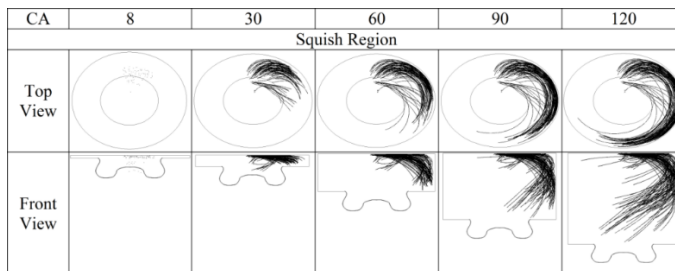


**Fig. 2. In-cylinder pathlines in the squish region.**

**4.2. Soot particle size distribution**

Figure 3 shows the distribution of soot particles in the whole cylinder with six different size ranges at crank angle 8, 30, 60, 90 and 120 degree ATDC. At 8° CA ATDC, a high concentration of soot can be observed inside cylinder bowl with a particle size in the range of 10-50 nm. As the combustion inside the cylinder continues, soot particle spread out to the entire cylinder thus reduce the concentration of soot particle spread and the size range increase from 2 nm up to 100 nm. At 30°

CA ATDC, soot particles start to move to squish region near the cylinder wall and the size of soot particles were about 20-50 nm while soot particle with a larger size will accumulate at the centre of the cylinder with an average size of 20-50 nm.

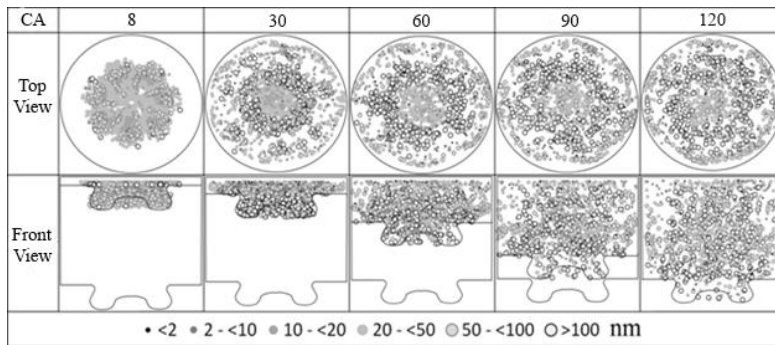


**Fig. 3. Soot particle size distribution in the whole cylinder.**

Figure 4 shows the soot particle size distribution in the squish region. The soot particles transported to the squish region near the cylinder wall was around 20-50 nm in size were originated from the centre of the cylinder. As the progression continues, soot particles scatter away from the centre of the cylinder toward the cylinder wall. The size range of soot particle widens from only 20-50 nm to 2-100 nm with an average of 43 nm at the end of the simulation.

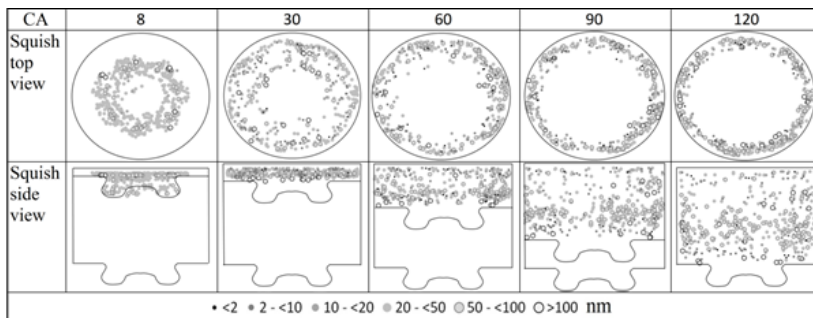


**Fig. 4. Soot particle size distribution inside the cylinder in the squish region.**

In the entire time of the simulation, primary soot particle size recorded in the whole cylinder was around 20-50 nm with average around 50 nm as in Fig. 5. The quantity of the primary particle size was reduced and scattered in all bins of ranges, especially at the later crank angles. A drastic increase in >100 nm range can be seen and was caused by the coagulation process where without coagulation process the primary size recorded in our previous paper was in the range of 10-20 nm [8]. This showed that coagulation process plays a huge role in increasing the soot particle size and reducing the soot number density.

Figure 6 shows the soot particle size distribution in squish region. At the start of the combustion, soot particle size distribution in squish region was in the range of 10 until up to more than 100 nm with the average size around 40 nm and high

frequency of soot particles were found in the size range of 20-50 nm. As the combustion continues, soot particle number in the range of 20-50 nm decreases almost half from the initial but maintains as the primary size range. The particles from the initial crank angles reduce in size particle due to oxidation and larger due to coagulation according to the history of the pathlines. Hence the frequency in others size ranges increase. Just before the exhaust valve opens (EVO), the soot particle average size show a maximum at 20-50 nm and 50-100 nm ranges.

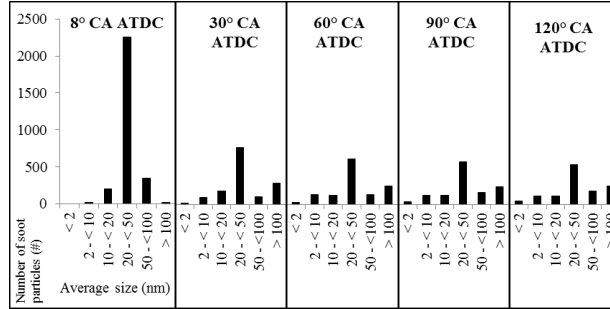


Fig. 5. Soot particle size distribution inside the whole cylinder.

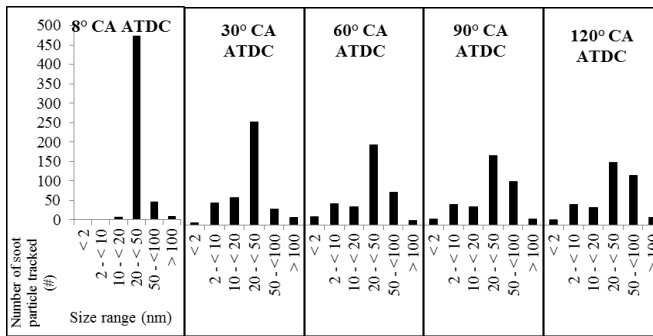
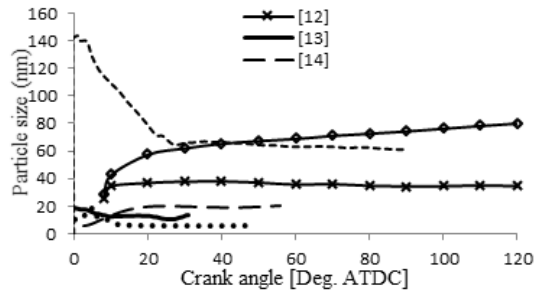


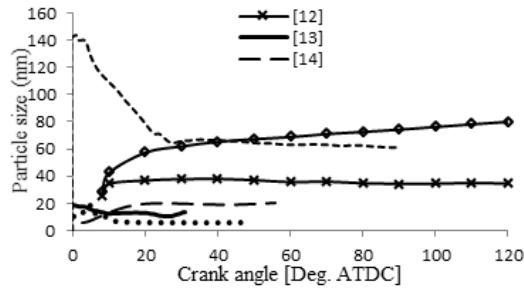
Fig. 6. Soot particle size distribution in squish region.

Figure 7 showed the soot particle size obtained in this work as compared with other research works [7-9, 14, 15]. The trends of soot particle size were very different between research because of the difference in simulation setup, parameter, model and technique used. But a steady change in soot particle can be found after a certain time in this case around 20° CA ATDC. As can be observed, the increase of soot particle size in this paper at the steady pace after 20° CA ATDC was due to the coagulation process. The increase in size without coagulation process as shown in Fig. 7, was labelled as [7], from the previous study. The surface growth and oxidation processes balanced each other hence resulted in an only small change in size when compared when coagulation process is included.

Statistically, in the early crank angle, soot particle number tracked and soot number density in the whole cylinder and squish region were the highest but as the combustion progress, both soot particle number and soot number density decreased until 20° CA ATDC as shown in Fig. 8. After that, the reduction of soot particle number tracked and soot number density reduces slowly until 120° CA ATDC.



**Fig. 7. Soot particle size comparison with other research works.**



**Fig. 8. Number of soot particle tracked and soot number density in squish region.**

There are various factors that influence the decrease in the number of soot particle tracked and soot number density in the diesel engine. The most common factors are in-cylinder temperature and in-cylinder pressure which affect the overall combustion and soot formation process. Higher pressure will promote a mixture of fuel and air while the higher temperature will promote fuel combustion.

Figure 9 shows that starting at 8° CA ATDC, the highest pressure and temperature were recorded. Higher pressure and temperature will promote combustion but due to the high concentration of fuel at that instant, more soot will also be produced. At the start of the combustion, the in-cylinder pressure drops rapidly until 60° CA ATDC but after that, it reduced slowly.

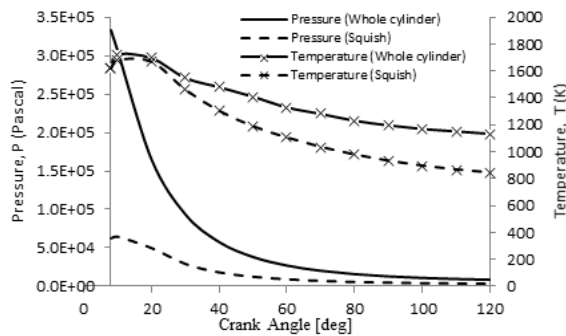


**Fig. 9. In-cylinder pressure and temperature in whole cylinder and squish region.**

## 5. Conclusions

The number of soot particles in the whole cylinder reduced drastically in the early crank angle until 30°CA ATDC and starts to flatten out as oxidation process slowed down and coagulation process picked up. Soot particles that accumulate in the squish region are about 10% of the whole in-cylinder soot particles. The particles vary in size but are mostly in the size range of 20 to 50 nm with the average size of 43 nm just before the exhaust valve opening. Soot particles in the range of 50 to 100 nm were significant in number as well. Looking at both graphical representation of the whole cylinder and squish region, it can be concluded that soot particle with smaller size than 50 nm tend to move near the cylinder wall and likely to be deposited into the lubricant while larger soot particles tend to accumulate at the centre of the cylinder and likely to be pushed out of the engine during the exhaust stroke. Results from the present study are similar to others' work and would be one of the methods to analysis soot particles in an engine.

## Acknowledgement

The authors would like to express their gratitude to the Ministry of Education of Malaysia and Universiti Kebangsaan Malaysia for supporting this research through FRGS/1/2013/TK01/UKM/02/2 research grant.

## References

1. Aldajah, S.; Ajayi, O.O.; Fenske, G.R.; and Goldblatt, I. L. (2007). Effect of exhaust gas recirculation (EGR) contamination of diesel engine oil on wear. *Wear*, 263(1), 93-98.
2. George, S.; Balla, S.; and Gautam, M. (2007). Effect of diesel soot contaminated oil on engine wear. *Wear*, 262, (9-10), 1113-1122.
3. George, S.; Balla, S.; Gautam, V.; and Gautam, M. (2007). Effect of diesel soot on lubricant oil viscosity. *Tribol. International*, 40(5), 809-818.
4. Tan, S.M.; Ng, H.K; and Gan, S. (2013). Computational study of crevice soot entrainment in a diesel engine. *Applied Energy - Barking then Oxford*, 102, 898-907.
5. Tan, S.M.; Ng, H.K; and Gan, S. (2013). CFD modelling of soot entrainment via thermophoretic deposition and crevice flow in a diesel engine. *Journal of Aerosol Science*, 66, 83-95.
6. Wan Mahmood, W.M.F.; LaRocca, A.; Shayler, P.J.; Pegg, I.; and Bonatesta, F. (2012). Predicted paths of soot particles in the cylinders of a direct injection diesel engine. *SAE International*, 2012-01-0148.
7. Zuber, M.A.; Wan Mahmood, W.M.F.; Abidin, Z.Z.; and Harun, Z. (2014). In-cylinder soot particle distribution in squish region of a direct injection diesel engine. *International Journal of Mechanical and Mechatronics Engineering*, 14(5), 51-58.
8. Zuber, M.A.; Wan Mahmood, W.M.F.; Harun, Z.; La Rocca, A.; and Shayler, P.J. (2015). Modeling of in-cylinder soot particle size evolution and distribution in a direct injection diesel engine. *SAE Technical Paper*, 2015-01-1075.

9. Rao, V.; and Honnery, D. (2014). Application of a multi-step soot model in a thermodynamic diesel engine model. *Fuel*, 135, 269-278.
10. Hiroyasu, H.; and Nishida, K. (1989). Simplified three-dimensional modeling of mixture formation and combustion in a D.I. diesel engine. *SAE Technical Paper*, 890269.
11. Fusco, A.; Knox-Kelecy, A.L.; and Foster, D.E.. (1994). Application of a phenomenological soot model for diesel engine combustion. Proceedings of the *Third International Symposium on Diagnostics and Modeling of Combustion in Internal Combustion Engine*. Yokohama, Japan, 571-576.
12. Tao, F.; Golovitchev, V.I.; and Chomiak, J. (2001). Application of complex chemistry to investigate the combustion zone structure of DI diesel sprays under engine-like condition. *Proceedings of the Fifth International Symposium on Diagnostics and Modeling of Combustion in Internal Combustion Engines*. Nagoya, Japan.
13. Wersborg, B.L.; Howard, J.B.; and Williams, G.C. (1973). Physical mechanisms in carbon formation in flames. *Symposium (International) on Combustion*, 14(1), 929-940.
14. Kazakov, A.; and Foster, D.E. (1998). Modeling of soot formation during diesel combustion using a multi-step phenomenological model. *SAE Technical Paper*, 982463.
15. Oh, K.C.; Lee, U.D.; Shin, H.D.; and Lee, E.J. (2005). The evolution of incipient soot particles in an inverse diffusion flame of ethene. *Combustion and Flame*, 140(3), 249-254.